


 Cite this: *Chem. Commun.*, 2024, 60, 8451

 Received 5th July 2024,  
 Accepted 11th July 2024

DOI: 10.1039/d4cc03354j

rsc.li/chemcomm

# Detection of diheptacendiyl diradical intermediate in the cycloreversion of diheptacene to heptacene†

 Marie S. Wagner,<sup>ab</sup> Heiko Peisert,<sup>id</sup> b Thomas Chassé<sup>b</sup> and Holger F. Bettinger<sup>id</sup> \*<sup>a</sup>

**Cycloreversion of diheptacenes, the covalently bound dimers of heptacene, in the solid state produces heptacene. In addition, diheptacendiyl diradical can be detected by ESR spectroscopy. The diradical has a small singlet–triplet energy gap of  $-0.02 \text{ kJ mol}^{-1}$  ( $-4.8 \times 10^{-3} \text{ kcal mol}^{-1}$ ) in favor of the singlet state and is persistent in solid heptacene.**

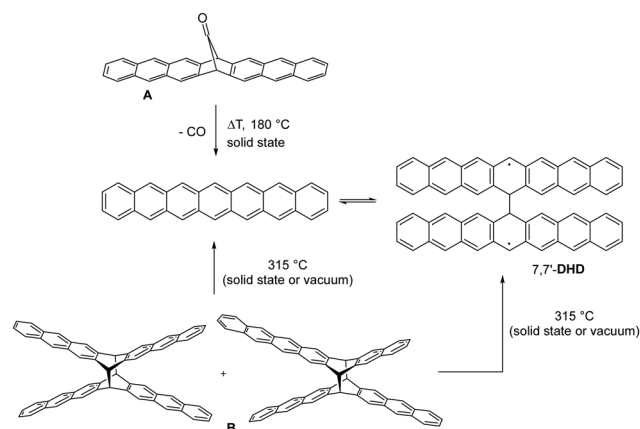
Heptacene is an organic semiconductor that can rival the well-established pentacene standard.<sup>1</sup> The problems associated with the inherently higher reactivity of heptacene can be mitigated by using a protected heptacene precursor that is transformed into heptacene *in situ*.<sup>1</sup> Currently, two suitable precursors are known for this purpose: 7,16-dihydro-7,16-methanoheptacene-19-one **A**<sup>1,2</sup> and the mixture of diheptacenes **B** (Scheme 1).<sup>3</sup> Heptacene can be obtained from **A** by photochemical or thermal CO extrusion in the solid state.<sup>1,2</sup> The covalent heptacene dimers **B** undergo cycloreversion to heptacene as shown by solution phase UV/vis and solid state NMR spectroscopy as well as UV/vis and IR spectroscopy under matrix isolation conditions after sublimation of the generated heptacene.<sup>3</sup> This approach allowed deposition of heptacene on coinage metal surfaces and its characterization by a multitude of surface science techniques, including “orbital tomography” and scanning tunneling microscopy, as well as action spectroscopy in helium nanodroplets.<sup>3–7</sup>

While the cheletropic extrusion of CO is allowed by the principle of orbital symmetry conservation, the  $[\pi 4_s + \pi 4_s]$  cycloreversion of diheptacenes **B** is forbidden under thermal conditions.<sup>8</sup> A stepwise cycloreversion is thus likely, and this is expected to involve a diradical intermediate, diheptacendiyl diradical (**DHD**) (see Scheme 1). This assumption was

substantiated by the computational investigation of heptacene dimerization.<sup>9</sup>

Recall that the photochemical  $[\pi 4_s + \pi 4_s]$  dimerization is an allowed reaction and an important photoreaction of acenes.<sup>10–12</sup> In a broader context, the thermal dimerization of acenes (and by the principle of microscopic reversibility their cycloreversion) is of substantial interest in the context of the pressure induced transition of graphite to diamond as well as the shock compression of aromatic systems.<sup>13,14</sup>

We here report the ESR spectroscopy detection of a diheptacendiyl diradical **DHD** in the solid state synthesis of heptacene by the cycloreversion of diheptacenes. The diradical has a very small singlet–triplet energy gap and is persistent in the heptacene solid. This is the first instance of the observation of an intermediate in the orbital symmetry forbidden thermal  $[\pi 4_s + \pi 4_s]$  cycloaddition/cycloreversion of heptacenes. The corresponding diradical was previously suggested to be involved in the photolysis of 1,2,3,4,5,6,7,8-octamethylantracene.<sup>15</sup>



**Scheme 1** Synthesis of heptacene from bridged monoketone precursor **A** or from mixture of diheptacenes **B**. For ease of representation, only one possible isomer of diheptacendiyl **DHD**, namely 7,7',16,16'-tetrahydro [7,7'-diheptacen]-16,16'-diyl (7,7'-**DHD**), is shown.

<sup>a</sup> Institute of Organic Chemistry, University of Tübingen, Auf der Morgenstelle 18, 72076 Tübingen, Germany. E-mail: holger.bettinger@uni-tuebingen.de

<sup>b</sup> Institute of Physical and Theoretical Chemistry, University of Tübingen, Auf der Morgenstelle 18, 72076 Tübingen, Germany

† Electronic supplementary information (ESI) available: Experimental details, discussion of zero-field splitting, half-field signal intensity, computational details, Cartesian coordinates. See DOI: <https://doi.org/10.1039/d4cc03354j>



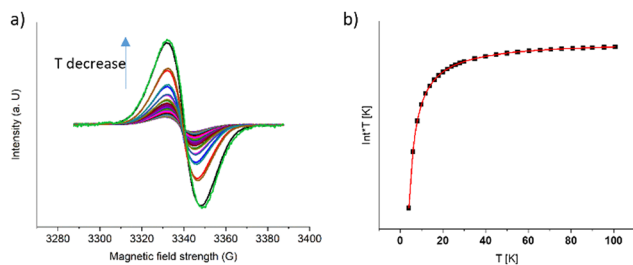


**Fig. 1** (a) Temperature dependent EPR signal of 7,7'-diheptacenyldiradical; signal intensity increases with decreasing temperature. (b) Plot of the product of integrated signal intensity and temperature  $T$  vs.  $T$ ; the red line is the fit to the data using the Bleaney–Bowers equation.

The diheptacene powder sample obtained after synthesis is diamagnetic and shows no ESR signal between 5–298 K. After heating the diheptacene precursor at 315 °C for 15 min, we were able to detect a signal at room temperature (Fig. 1, see ESI,† Fig. S1 for an enlargement). Keeping the sample at room temperature, the signal intensity increases until it has reached its maximum after 5–6 hours. The next day and even several weeks later, no change in intensity was observed. We assign this signal to an organic diradical based on the chemical shift and the observed temperature dependence of the signal intensity (Fig. 1a and b).<sup>16</sup> Note that the signal intensity of doublet radicals is not temperature dependent.<sup>16</sup> The observed signal does not show zero-field splitting (ZFS), which is explained by the expected small  $|D|$  value of the most stable rotamer of the diradical (see below and ESI†). Due to the small  $|D|$  value also no half-field signal could be detected (see ESI† for a more detailed discussion and simulated ESR spectra).

The signal intensity shows pronounced temperature dependence (Fig. 1a) that was reversible in the temperature range 4–298 K. Mathematically, the temperature dependence of the ESR signal intensity of triplet diradicals can be described using the Bleaney–Bowers equation (see ESI†).<sup>16,17</sup> The signal intensity increases at low temperatures (Fig. 1a) and when plotting the product of intensity and temperature ( $\text{Int} \cdot T$ ) against  $T$  for temperatures between 4–100 K, we obtained non-linear behavior (Fig. 1b). This is evidence of a singlet ground state with a very small energy gap between triplet and singlet states. Through a fit procedure we determined a value of  $\Delta E_{\text{ST}} = -0.02 \text{ kJ mol}^{-1}$  ( $-4.8 \times 10^{-3} \text{ kcal mol}^{-1}$ ) for the singlet–triplet energy gap in favor of the singlet state (see ESI†).

The previous investigation of the solid-state cycloreversion of diheptacenes could measure a solid state  $^{13}\text{C}$  cross-polarization magic angle spinning (CP-MAS) NMR spectrum of the resulting solid heptacene sample after heating of the diheptacene sample.<sup>3</sup> As the ESR method is very sensitive to the presence of low concentrations of radical species, the NMR spectrum may not be affected by the presence of diradicals provided their concentration is low. Indeed, transferring the sample into a solid-state NMR spectrometer gave the  $^{13}\text{C}$ -CP-MAS spectrum of heptacene as reported previously.<sup>3</sup>

Heptacene itself can be excluded as the detected ESR active species as heptacene photogenerated from the  $\alpha$ -diketone

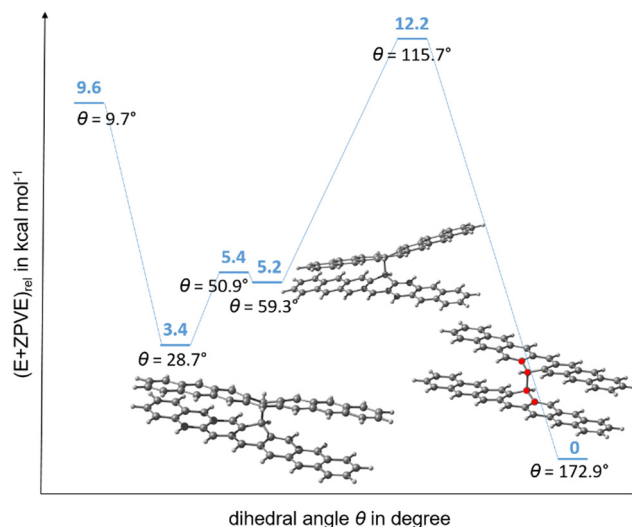


**Fig. 2** Zero-point vibrational energy (ZPVE) corrected potential energy diagram ( $E_0$  in  $\text{kcal mol}^{-1}$ ) for rotation of the two heptacenyldiradical wings of the triplet state of 7,7'-DHD as computed at the M06-2X/def2-SVP level of theory. The dihedral angle  $\theta$  involving the red atoms is given in degree.

precursor is ESR silent in an argon matrix.<sup>18</sup> In addition, the singlet–triplet energy gap of heptacene is expected to be much larger than  $5 \text{ cal mol}^{-1}$  based on available computational data that arrive at gaps ranging between 9–12  $\text{kcal mol}^{-1}$ .<sup>3,19–22</sup>

A more likely carrier of the diradical signal is the diheptacenyldiradical DHD. This assumption can be substantiated using computational chemistry methods with a focus on the centrosymmetric diheptacene isomer. The data for the lower symmetry 6,7'-DHD isomer are very similar and can be found in the ESI.† After breaking of one C–C single bond between bridgehead carbon atoms, the resulting 7,7'-diheptacenyldiradical (7,7'-DHD) was treated in its triplet electronic state using the M06-2X/def2-SVP method. A scan of the potential energy surface around the dihedral angle involving the remaining C–C single bond revealed three local minima and three local maxima (see ESI,† Fig. S8). Their structures were subsequently fully optimized (Fig. 2). The most stable minimum has a large dihedral angle of  $173^\circ$ , while the others have smaller dihedral angles and are about  $3 \text{ kcal mol}^{-1}$  (dihedral angle of  $29^\circ$ ) and  $5 \text{ kcal mol}^{-1}$  (dihedral angle of  $59^\circ$ ) higher in energy. A very small energy barrier of  $0.2 \text{ kcal mol}^{-1}$  with respect to the higher energy rotamer interconnects the latter two rotamers. The most stable rotamer represents the most significant structural distortion compared to diheptacene as the two heptacene moieties are in an anti arrangement.

The geometry and the energy of the singlet state of the diradical computed using the symmetry broken approach (UM06-2X/def2-SVP) are quite similar to that of the triplet state. The difference in energy is merely  $0.1 \text{ kcal mol}^{-1}$  in favor of the singlet state in qualitative agreement with experiment. The essentially isoenergetic nature of the singlet and triplet state is confirmed by more sophisticated strongly contracted  $N$ -electron valence state perturbation theory (SC-NEVPT2/def2-SVP) computations based on a CASSCF(10,10) wavefunction.



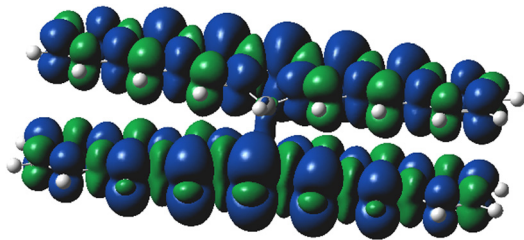


Fig. 3 Computed (UM06-2X/def2-SVP) spin-density of the most stable rotamer of 7,7'-DHD.

While the singlet state is lowest in energy for the most stable conformer with  $173^\circ$  dihedral angle, this ordering is reversed for the next higher conformer (dihedral angle of  $29^\circ$ ). The energy differences between the electronic states are, however, less than  $0.1 \text{ kcal mol}^{-1}$ . The computational analysis shows convincingly that the 7,7'-diheptacene diradical (and by analogy the 6,7'-diheptacene diradical) are very reasonable carriers of the observed ESR signal.

Conformers with small dihedral angle are expected to readily collapse to dimer **B** after intersystem crossing from the triplet to the singlet state. The barrier for this process was computed to be less than  $1 \text{ kcal mol}^{-1}$  by Bendikov *et al.*<sup>9</sup> As the diradical species is persistent at room temperature in the solid for a long time, we conclude that the conformer with the large dihedral angle of  $173^\circ$  is the most likely carrier of the ESR signal. The barrier for rotation about the C–C single bond is sizeable (about  $12 \text{ kcal mol}^{-1}$ , see Fig. 2) and the rotation is likely strongly restricted by the solid state environment of the diradical causing a much larger barrier than derived from our gas phase computations.<sup>23</sup> The computed spin-density shows strong delocalization (Fig. 3), and the computed  $|D|$  value<sup>24</sup> for this rotamer is indeed very low (see ESI,<sup>†</sup> also for 6,7'-DHD), in agreement with the lack of ZFS and half-field signal in the measured spectra.

In summary, the diheptacene diradical was detected by ESR spectroscopy of the heated diheptacene powder and has a very small singlet–triplet energy splitting of  $-0.02 \text{ kJ mol}^{-1}$  in favor of the singlet state based on the temperature dependence of the ESR signal intensity. The diradical is persistent in the solid heptacene matrix at room temperature for a long time. This is the first observation of an intermediate in the orbital symmetry forbidden thermal dimerization of heptacene, which confirms previous computational analyses of thermal acene dimerizations or cycloreversions of acene dimers.<sup>9</sup>

M. S. W. performed investigations and edited the manuscript; H. P. and T. C. edited the manuscript; H. F. B. conceptualized the study, performed investigations, provided resources, and wrote the manuscript. All authors edited the manuscript.

The authors acknowledge support by the state of Baden-Württemberg through bwHPC and the German Research Foundation (DFG) through grant no INST 40/575-1 FUGG (JUSTUS 2 cluster). We thank Dominik Brzecki for measuring

the EPR spectra, Dr Ralf Einholz and Virinder Bhagat for technical assistance, Prof. Kenji Matsuda, Prof. Manabu Abe, and Prof. Joris van Slageren for discussion and helpful comments.

## Data availability

The experimental and computational data of this manuscript are included in the ESI.<sup>†</sup>

## Conflicts of interest

There are no conflicts to declare.

## Notes and references

- 1 T. Miyazaki, M. Watanabe, T. Matsushima, C.-T. Chien, C. Adachi, S.-S. Sun, H. Furuta and T. J. Chow, *Chem. – Eur. J.*, 2021, **27**, 10677–10684.
- 2 M. Watanabe, Y. J. Chang, S.-W. Liu, T.-H. Chao, K. Goto, M. Minarul Islam, C.-H. Yuan, Y.-T. Tao, T. Shinmyozu and T. J. Chow, *Nat. Chem.*, 2012, **4**, 574–578.
- 3 R. Einholz, T. Fang, R. Berger, P. Grüninger, A. Früh, T. Chassé, R. F. Fink and H. F. Bettinger, *J. Am. Chem. Soc.*, 2017, **139**, 4435–4442.
- 4 M. S. Sättele, A. Windischbacher, L. Egger, A. Haags, P. Hurdax, H. Kirschner, A. Gottwald, M. Richter, F. C. Bocquet, S. Soubatch, F. S. Tautz, H. F. Bettinger, H. Peisert, T. Chassé, M. G. Ramsey, P. Puschnig and G. Koller, *J. Phys. Chem. C*, 2021, **125**, 2918–2925.
- 5 T. G. Boné, A. Windischbacher, M. S. Sättele, K. Greulich, L. Egger, T. Jauk, F. Lackner, H. F. Bettinger, H. Peisert, T. Chassé, M. G. Ramsey, M. Sterrer, G. Koller and P. Puschnig, *J. Phys. Chem. C*, 2021, **125**, 9129–9137.
- 6 T. Boné, A. Windischbacher, L. Scheucher, F. Presel, P. Schnabl, M. S. Wagner, H. F. Bettinger, H. Peisert, T. Chassé, P. Puschnig, M. G. Ramsey, M. Sterrer and G. Koller, *J. Phys.: Condens. Matter*, 2023, **35**, 475003.
- 7 M. Kappe, A. Schiller, F. Zappa, S. A. Krasnokutski, M. S. Wagner, H. F. Bettinger and P. Scheier, *Astron. Astrophys.*, 2023, **672**, A4.
- 8 R. B. Woodward and R. Hoffmann, *Angew. Chem., Int. Ed. Engl.*, 1969, **8**, 781–853.
- 9 S. S. Zade, N. Zamoshchik, A. R. Reddy, G. Fridman-Marueli, D. Sheberla and M. Bendikov, *J. Am. Chem. Soc.*, 2011, **133**, 10803–10816.
- 10 S. M. Sieburth and N. T. Cunard, *Tetrahedron*, 1996, **52**, 6251–6282.
- 11 G. Kaupp, *Angew. Chem., Int. Ed. Engl.*, 1992, **31**, 422–424.
- 12 H. Bouas-Laurent and J. P. Desvergne, in *Photochromism*, ed. H. Dürr and H. Bouas-Laurent, Elsevier Science, Amsterdam, 2003, pp. 561–630, DOI: [10.1016/B978-044451322-9/50018-X](https://doi.org/10.1016/B978-044451322-9/50018-X).
- 13 B. Slepetz and M. Kertesz, *J. Am. Chem. Soc.*, 2013, **135**, 13720–13727.
- 14 J. Quenneville and T. C. Germann, *J. Chem. Phys.*, 2009, **131**, 024313.
- 15 M. A. Meador and H. Hart, *J. Org. Chem.*, 1989, **54**, 2336.
- 16 M. Abe, *Chem. Rev.*, 2013, **113**, 7011–7088.
- 17 B. Bleaney and K. D. Bowers, *Proc. R. Soc. Lond. A*, 1952, **214**, 451–465.
- 18 H. F. Bettinger, R. Mondal and D. C. Neckers, *Chem. Commun.*, 2007, 5209–5211.
- 19 B. Hajgato, M. Huzak and M. S. Deleuze, *J. Phys. Chem. A*, 2011, **115**, 9282–9293.
- 20 J.-D. Chai, *J. Chem. Phys.*, 2014, **140**, 18A521.
- 21 Y. Yang, E. R. Davidson and W. Yang, *Proc. Natl. Acad. Sci. U. S. A.*, 2016, **113**, E5098–E5107.
- 22 J.-D. Chai, *J. Chem. Phys.*, 2017, **146**, 044102.
- 23 B. H. Northrop, J. E. Norton and K. N. Houk, *J. Am. Chem. Soc.*, 2007, **129**, 6536–6546.
- 24 S. Sinnecker and F. Neese, *J. Phys. Chem. A*, 2006, **110**, 12267–12275.

